RevMexAA (Serie de Conferencias), **27**, 240–244 (2007)

LAUNCHING OF POYNTING JETS FROM ACCRETION DISKS

R. V. E. Lovelace[1] and M. M. Romanova[1]

RESUMEN

Es posible que los chorros que se originan en objetos compactos que acretan gas sean producidos por la torsión de líneas de campo magnético ancladas en un disco de acreción con rotación diferencial, extrayendo así energía y momento angular del mismo. Se han discutido dos opciones en general: flujos hidromagnéticos, que llevan una masa considerable y donde tanto la energía, como el momento angular, son llevados por masa y campo electromagnético, y flujos de Poynting, donde el flujo de masa es despreciable y la energía y el momento angular son transportados por el campo electromagnético. Describimos aquí trabajo teórico reciente sobre la formación de chorros de Poynting relativistas de discos de acreción magnetizados, así como nuevas simulaciones (de partícula en una celda) de la formación de chorros a partir de discos.

ABSTRACT

The jets observed to emanate from many compact accreting objects may arise from the twisting of the magnetic field threading a differentially rotating accretion disk which acts to magnetically extract angular momentum and energy from the disk. Two main regimes have been discussed, hydromagnetic outflows, which have a significant mass flux and have energy and angular momentum carried by both matter and electromagnetic field and, Poynting outflows, where the mass flux is negligible and energy and angular momentum are carried predominantly by the electromagnetic field. We describe recent theoretical work on the formation of relativistic Poynting jets from magnetized accretion disks and new relativistic, fully-electromagnetic, particle-in-cell simulations of the formation of jets from accretion disks.

Key Words: **GALAXIES: ACTIVE — GALAXIES: JETS — MAGNETIC FIELDS — QUASARS**

1. GENERAL

Powerful, highly-collimated, oppositely directed jets are observed in active galaxies and quasars, and in old compact stars in binaries - the 'micro-quasars'. Different models have been put forward to explain astrophysical jets (Bisnovatyi-Kogan & Lovelace 2001). Recent observational and theoretical work favors models where twisting of an ordered magnetic field threading an accretion disk acts to magnetically accelerate the jets. Two main regimes have been considered in theoretical models, the hydromagnetic regime where the energy and angular momentum is carried by both the electromagnetic field and the kinetic flux of matter, and the Poynting flux regime where the energy and angular momentum outflow from the disk is carried predominantly by the electromagnetic field. In §3 we outline the theory of Poynting jets. In §4 we present new results from axisymmetric, fully electromagnetic, relativistic-particle-in-cell (PIC) simulations of the formation and propagation of relativistic jets from a disk.

2. THEORY OF POYNTING JETS

The powerful jets observed from active galaxies and quasars are probably not hydromagnetic outflows but rather Poynting flux dominated jets. The motion of these jets measured by very long baseline interferometry correspond to bulk Lorentz factors of $\Gamma = \mathcal{O}(10)$ which is much larger than the Lorentz factor of the Keplerian disk velocity predicted for hydromagnetic outflows. Furthermore, the low Faraday rotation measures observed for these jets at distances $<$ kpc from the central object implies a very low plasma densities. Similar arguments indicate that the jets of microquasars are not hydromagnetic outflows but rather Poynting jets. Poynting Jets have been proposed to be the driving mechanism for gamma ray burst sources (Katz 1997). Theoretical studies have developed models for Poynting jets from accretion disks (Lovelace, Wang, & Sulkanen 1987; Lynden-Bell 2003; Romanova & Lovelace 1997; Levinson 1998; Lovelace et al. 2002; Lovelace & Romanova 2003). Stationary Poynting flux dominated outflows were found by Romanova et al. (1998) and Ustyugova et al. (2000) in axisymmetric MHD simulations of the opening of magnetic loops threading a Keplerian disk.

[1] Cornell University, Ithaca, NY, USA.

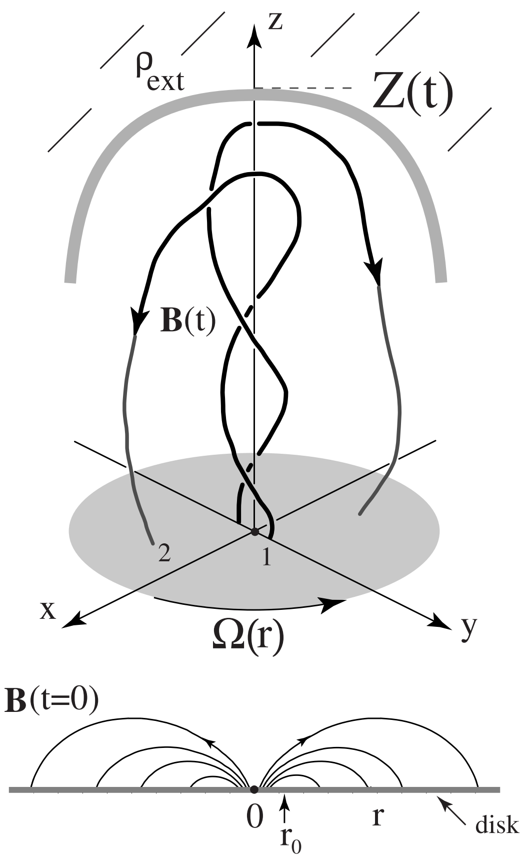

Fig. 1. Sketch of the magnetic field configuration of a Poynting jet from Lovelace & Romanova (2003). The bottom part of the figure shows the initial dipole-like magnetic field threading the disk which rotates at the angular rate $\Omega(r)$. The top part of the figure shows the jet at some time later when the head of the jet is at a distance $Z(t)$. At the head of the jet there is force balance between electromagnetic stress of the jet and the ram pressure of the ambient medium of density ρ_{ext}.

We first summarize the theory of non-relativistic Poynting jets which is based on the Grad-Shafranov equation. We show results of non-relativistic, axisymmetric MHD simulations which support this theory. Later, we discuss the corresponding results obtained by solving the relativistic Grad-Shafranov equation.

Consider the coronal magnetic field - such as that shown in the lower part of Figure 1 - of a differentially rotating Keplerian accretion disk. That is, the disk is perfectly conducting, high-density, and has a small accretion speed ($\ll v_K$). Further, consider "coronal" or "force-free" magnetic fields in the non-relativistic limit. We use cylindrical (r, ϕ, z) coordinates and consider axisymmetric field configurations. Thus the magnetic field has the form $\mathbf{B} = \mathbf{B}_p + B_\phi \hat{\boldsymbol{\phi}}$, with $\mathbf{B}_p = B_r \hat{\mathbf{r}} + B_z \hat{\mathbf{z}}$. Because $\nabla \cdot \mathbf{B} = 0$, $\mathbf{B} = \nabla \times \mathbf{A}$ with $\mathbf{A}$ the vector potential. Consequently, $B_r = -(1/r)\partial\Psi/\partial z$ and $B_z = (1/r)\partial\Psi/\partial r$. where $\Psi(r, z) \equiv rA_\phi(r, z)$. The $\Psi(r, z) =$ const lines label the poloidal field lines; that is, $(\mathbf{B}_p \cdot \nabla)\Psi = 0 = (\mathbf{B} \cdot \nabla)\Psi$. Note that $2\pi\Psi(r, z)$ is the magnetic flux through a horizontal, coaxial circular disk of radius r. The magnetic field threading the disk at $z = 0$ is assumed to evolve slowly so that it can be considered approximately time-independent, $\Psi(r, z = 0) = \Psi_0(r)$. However, the magnetic field above the disk will in general be time-dependent, $\Psi = \Psi(r, z, t)$, due to the differential rotation of the disk.

The non-relativistic equation of plasma motion in the corona of an accretion disk is $\rho d\mathbf{v}/dt = -\nabla p + \rho\mathbf{g} + \mathbf{J} \times \mathbf{B}/c$, where $\mathbf{v}$ is the flow velocity, p is the pressure, and $\mathbf{g}$ is the gravitational acceleration. The equation for the $\mathbf{B}$ field is $\nabla \times \mathbf{B} = 4\pi\mathbf{J}/c$, because the displacement current is negligible in the non-relativistic limit. In the coronal or force-free plasma limit, the magnetic energy density $\mathbf{B}^2/8\pi$ is much larger than the kinetic or thermal energy densities; that is, we have sub-Alfvénic flow speeds $\mathbf{v}^2 \ll v_A^2 = \mathbf{B}^2/(4\pi\rho)$, where v_A is the Alfvén velocity. The force equation then simplifies to $0 \approx \mathbf{J} \times \mathbf{B}$ so that $\mathbf{J} = \lambda\mathbf{B}$ (Gold & Hoyle 1960). Because $\nabla \cdot \mathbf{J} = 0$, $(\mathbf{B} \cdot \nabla)\lambda = 0$, and consequently $\lambda = \lambda(\Psi)$, as well-known. Thus Ampère's law becomes $\nabla \times \mathbf{B} = 4\pi\lambda(\Psi)\mathbf{B}/c$. The r and z components of this equation imply $rB_\phi = H(\Psi)$, and $dH(\Psi)/d\Psi = 4\pi\lambda(\Psi)/c$, where $H(\Psi)$ is another function of Ψ. Thus, $H(\Psi) =$ const are lines of constant poloidal current density; $\mathbf{J}_p = (c/4\pi)(dH/d\Psi)\mathbf{B}_p$ so that $(\mathbf{J}_p \cdot \nabla)H = 0$. The toroidal component of Ampère s law gives the non-relativistic Grad-Shafranov equation for Ψ,

$$\Delta^*\Psi = -H(\Psi)\frac{dH(\Psi)}{d\Psi} \ . \tag{1}$$

Here, $\Delta^* \equiv \partial^2/\partial r^2 - (1/r)(\partial/\partial r) + \partial^2/\partial z^2$ is the adjoint Laplacian operator. Note that $\Delta^*\Psi = r(\nabla^2 - 1/r^2)A_\phi$ and that $H(dH/d\Psi) = 4\pi rJ_\phi/c$. From Ampère's law, $\oint d\mathbf{l} \cdot \mathbf{B} = (4\pi/c)\int d\mathbf{S} \cdot \mathbf{J}$, so that $rB_\phi(r, z) = H(\Psi)$ is $(2/c)$ times the current flowing through a circular area of radius r (with normal $\hat{\mathbf{z}}$) labeled by $\Psi(r, z) =$ const. Equivalently, $-H[\Psi(r, 0)]$ is $(2/c)\times$ the current flowing into the area of the disk with radii $\leq r$. For all cases studied here, $-H(\Psi)$ has a maximum so that the total current flowing into the disk for $r \leq r_m$ is $I = (2/c)(-H)_{max}$, where r_m is such that $-H[\Psi(r_m, 0)] = (-H)_{max}$ so that r_m is less than the radius of the O-point, r_0. The same total current I_{tot} flows out of the region of the disk $r = r_m$ to r_0.

The function $H(\Psi)$ must be determined before the Grad-Shafranov equation can be solved. $H(\Psi)$ is determined by the differential rotation of the disk: The azimuthal twist of a given field line going from an inner footpoint at r_1 to an outer footpoint at r_2 is fixed by the differential rotation of the disk. The field line slippage speed through the disk due to the disk's finite magnetic diffusivity is estimated to be negligible compared with the Keplerian velocity v_K. For a given field line we have $r d\phi/B_\phi = ds_p/B_p$, where $ds_p = \sqrt{dr^2 + dz^2}$ is the poloidal arc length along the field line, and $B_p = \sqrt{B_r^2 + B_z^2}$. The total twist of a field line loop is

$$\Delta\phi(\Psi) = -\int_1^2 ds_p \ \frac{B_\phi}{rB_p} = -H(\Psi)\int_1^2 \frac{ds_p}{r^2 B_p} \ , \quad (2)$$

with the sign included to give $\Delta\phi > 0$. For a Keplerian disk around an object of mass M, the angular rotation rate is $\Omega_K = \sqrt{GM/r^3}$ so that the field line twist after a time t is $\Delta\phi(\Psi) = \Omega_0 t\big[(r_0/r_1)^{3/2} - (r_0/r_2)^{3/2}\big] = (\Omega_0 t)F(\Psi/\Psi_0)$, where r_0 is the radius of the O-point, $\Omega_0 = \sqrt{GM/r_0^3}$, and F is a dimensionless function.

Equations (1) and (2) have been solved numerically by Li et al. (2001) and Lovelace et al. (2002) for an initial poloidal magnetic field as shown in the lower part of Figure 1. As the "twist," as measured by $\Omega_0 t$, increases, a high twist field configuration appears with a different topology. A "plasmoid" consisting of toroidal flux detaches from the disk and propagates outward. The plasmoid is bounded by a poloidal field line which has an X-point above the O-point on the disk. The occurrence of the X-point requires that there be at least a small amount of dissipation in the evolution from the poloidal dipole field and the Poynting jet configuration. The high-twist configuration consists of a region near the axis which is magnetically collimated by the toroidal B_ϕ field and a region far from the axis which is anti-collimated in the sense that it is pushed away from the axis. The field lines returning to the disk at $r > r_0$ are anti-collimated by the pressure of the toroidal magnetic field. The poloidal field fills only a small fraction of the coronal space.

Figure 2 shows results of non-relativistic axisymmetric simulations of the formation of a Poynting jet by Ustyugova et al. (2000). The flow near the $z-$axis is the Poynting jet and its physical properties agree with Grad-Shafranov solutions.

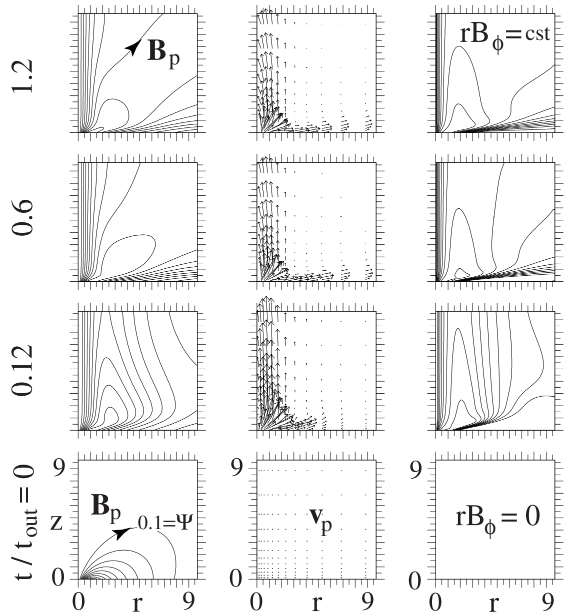

Fig. 2. Non-relativistic time evolution of dipole-like field threading the disk from the initial configuration $t = 0$ (bottom panels) to the final quasi-stationary state at $t = 1.2t_{out}$, where t_{out} is the rotation period of the disk at the outer radius R_{out} of the simulation region from Ustyugova et al. (2000). The left hand panels show the poloidal field lines which are the same as the $\Psi(r, z)$ =const lines; Ψ is normalized by Ψ_{max}, and the spacing between lines is 0.1. The middle panels show the poloidal velocity vectors $\mathbf{v}_p$. The right-hand panels show the constant lines of $-rB_\phi(r, z) > 0$ in units of Ψ_{max}/r_0, and the spacing between lines is 0.1. For this calculation a 100×100 inhomogeneous grid was used with Δr_j and Δz_k growing with distance r and z geometrically as $\Delta r_j = \Delta r_1 q^j$ and $\Delta z_k = \Delta z_1 q^k$, with $q = 1.03$ and $\Delta r_1 = \Delta z_1 = 0.05 r_0$.

In the case of relativistic Poynting jets we hypothesize that the magnetic field configuration is similar to that in the non-relativistic limit (Ustyugova et al. 2000; Lovelace et al. 2002). Thus, most of the twist $\Delta\phi$ of a field line of the relativistic Poynting jet occurs along the jet from $z = 0$ to $Z(t)$ as sketched in Figure 3, where $Z(t)$ is the axial location of the "head" of the jet. Along most of the distance $z = 0$ to Z, the radius of the jet is a constant and $\Psi = \Psi(r)$ for $Z >> r_0$. Note that the function $\Psi(r)$ is different from $\Psi(r, 0)$ which is the flux function profile on the disk surface. Hence $r^2 d\phi/dz = rB_\phi(r, z)/B_z(r, z)$. We take for simplicity $V_z = dZ/dt =$ const. We determine V_z subsequently. In this case $H(\Psi) = [r^2\Omega(\Psi)/V_z]B_z$ can be written as a function of Ψ and $d\Psi/dr$. With H

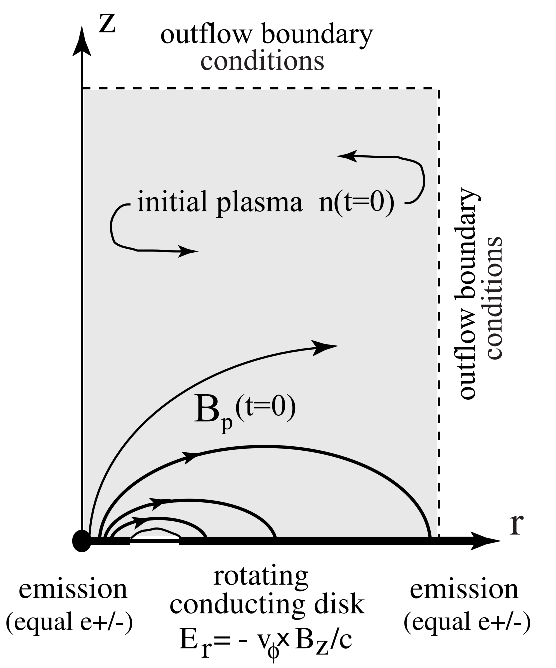

Fig. 3. Sketch of the initial conditions for the relativistic particle-in-cell simulations of jet formation from an accretion disk.

known, the relativistic Grad-Shafranov equation,

$$\left[1-\left(\frac{r\Omega}{c}\right)^2\right]\Delta^*\Psi-\frac{\nabla\Psi}{2r^2}\cdot\nabla\left(\frac{r^4\Omega^2}{c^2}\right)=-H(\Psi)\frac{dH(\Psi)}{d\Psi}, \tag{3}$$

can be solved (Lovelace & Romanova 2003).

The quantity not determined by equation (3) is the velocity V_z, or Lorentz factor $\Gamma = 1/(1 - V_z^2/c^2)^{1/2}$. This is determined by taking into account the balance of axial forces at the head of the jet: the electromagnetic pressure within the jet is balanced against the dynamic pressure of the external medium which is assumed uniform with density ρ_{ext}. This gives $(\Gamma^2 - 1)^3 = B_0^2/(8\pi\mathcal{R}^2\rho_{ext}c^2)$, or for $\Gamma \gg 1$,

$$\Gamma \approx 8\left(\frac{10}{\mathcal{R}}\right)^{1/3}\left(\frac{B_0}{10^3\mathrm{G}}\right)^{1/3}\left(\frac{1/\mathrm{cm}^3}{n_{ext}}\right)^{1/6}, \tag{4}$$

where $\mathcal{R} = r_0/r_g \gg 1$, with r_0 the O-point of the magnetic field, $r_g \equiv GM/c^2$, and B_0 the magnetic field strength at the center of the disk. This value of Γ is of the order of the Lorentz factors of the expansion of parsec-scale extragalactic radio jets observed with very-long-baseline-interferometry (see, e.g., Zensus et al. 1998). This interpretation assumes that the radiating electrons (and/or positrons) are accelerated to high Lorentz factors ($\gamma \sim 10^3$) at the jet front and move with a bulk Lorentz factor Γ relative to the observer. The luminosity of the $+z$ Poynting jet is $\dot{E}_j = c\int_0^{r_2} rdrE_rB_\phi/2 = cB_0^2\mathcal{R}^{3/2}r_g^2/3 \sim 2.1\times10^{46}(B_0/10^3\mathrm{G})^2(\mathcal{R}/10)^{3/2}(M/10^9M_\odot)^2$ erg/s, where M is the mass of the black hole.

For long time-scales, the Poynting jet is of course time-dependent due to the angular momentum it extracts from the inner disk ($r < r_0$) which in turn causes r_0 to decrease with time (Lovelace et al. 2002). This loss of angular momentum leads to a "global magnetic instability" and collapse of the inner disk (Lovelace et al. 1994, 1997, 2002) and a corresponding outburst of energy in the jets from the two sides of the disk. Such outbursts may explain the flares of active galactic nuclei blazar sources (Romanova & Lovelace 1997; Levinson 1998) and the one-time outbursts of gamma ray burst sources (Katz 1997).

3. RELATIVISTIC PARTICLE-IN-CELL SIMULATIONS OF JETS

We performed relativistic, fully electromagnetic, particle-in-cell simulations of the formation of relativistic jets from an accretion disk initially threaded by a dipole-like magnetic field. This was done using the code XOOPIC developed by Verboncoeur, Langdon, and Gladd (1995). Earlier, Gisler, Lovelace, and Norman (1989) studied jet formation for a monopole type field using the relativistic PIC code ISIS. The geometry of the initial configuration is shown in Figure 3. The computational region is a cylindrical "can," $r = 0 - R_m$ and $z = 0 - Z_m$, with outflow boundary conditions on the outer boundaries, and the potential and particle emission specified on the disk surface $r = 0 - R_m$, $z = 0$. Equal fluxes of electrons and positrons are emitted so that the net emission is effectively space-charge-limited. About 10^5 particles were used in the simulations reported here. The behavior of the lower half-space ($z < 0$) is expected to be a mirror image of the upper half-space.

Figure 4 shows the formation of a relativistic jet. The gray scale indicates the logarithm of the density of electrons or positrons with 20 levels between the lightest (10^{12}) and darkest ($4\times10^{15}/\mathrm{m}^3$). The lines are poloidal magnetic field lines $\mathbf{B}_p$. The total, three-dimensional magnetic field is shown in Figure 5. The computational region has $(R_m, Z_m) = (50, 100)$ m, the initial $\mathbf{B}-$field is dipole-like with $B_z(0,0) \equiv B_0 = 28.3$ G and an O-point at $(r,z) = (10,0)$ m, and the electric potential at the center of

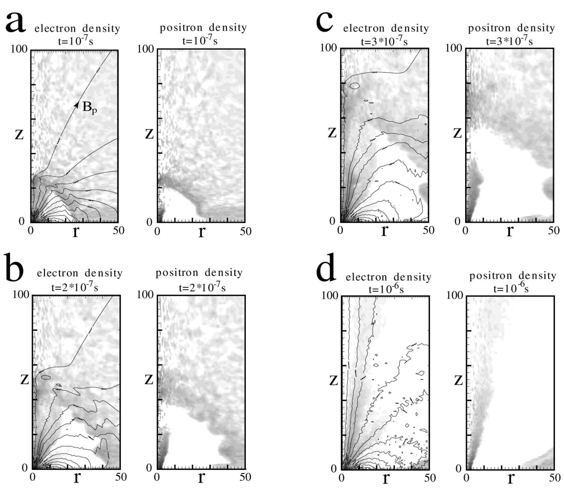

Fig. 4. Relativistic particle-in-cell simulations of the formation of a jet from a rotating disk. (a)-(c) give snapshots at times $(1, 2, 3) \times 10^{-7}$ s, and (d) is at $t = 10^{-6}$ s.

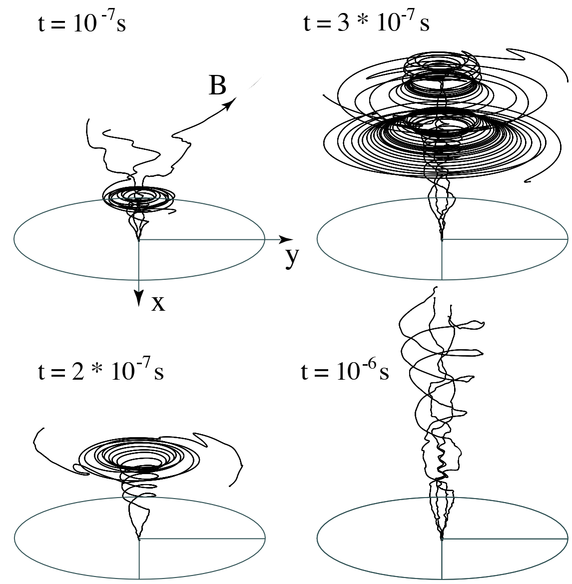

Fig. 5. Three dimensional magnetic field lines originating from the disk at $r = 1,\ 2$ m for the same case as Figure 4.

the disk is $\Phi_0 = -10^7$ V relative to the outer region of the disk. Initially, the computational region was filled with a distribution of equal densities of electrons and positrons with $n_{\pm}(0,0) = 3 \times 10^{13}/\mathrm{m}^3$. Electrons and positrons are emitted with equal currents $I_{\pm} = 3 \times 10^5$ A from both the inner and the outer portions of the disk as indicated in Figure 3 with an axial speed much less than c. For a Keplerian disk with $r_0 \gg r_g$, the scalings are $\Phi_0 \sim B_0(r_0 r_g)^{1/2}$, $I \sim cB_0 r_0$ and the jet power is $\sim cB_0^2 r_0^{3/2} r_g^{1/2}$. The calculations were done on a 64×128 grid stretched in both the r and z directions so as to give much higher spatial resolution at small r and small z. These simulations show the formation of a quasi-stationary, collimated current-carrying jet. The Poynting flux power of the jet is $\dot{E}_j \approx 7 \times 10^{11}$ W and the particle kinetic energy power is $\approx 4.7 \times 10^{10}$ W. The charge density of the electron flow is partially neutralized by the positron flow. Simulations are planned with the positrons replaced by ions.

We thank the meeting organizers for the stimulating and very well organized meeting. This work was supported in part by DOE cooperative agreement DE-FC03 02NA00057.

REFERENCES

Bisnovatyi-Kogan, G. S., & Lovelace, R. V. E. 2001, NewARev, 45, 663

Gisler, G., Lovelace, R. V. E., & Norman, M. L. 1989, ApJ, 342, 135

Gold, T., & Hoyle, F. 1960, MNRAS, 120, 89

Katz, J. I. 1997, ApJ, 490, 633

Levinson, A. 1998, ApJ, 507, 145

Lovelace, R. V. E., Berk, H. L., & Contopoulos, J. 1991, ApJ, 379, 696

Lovelace, R. V. E., Li, H., Koldoba, A. V., Ustyugova, G. V., & Romanova, M. M. 2002, ApJ, 572, 445

Lovelace, R. V. E., Newman, W. I., & Romanova, M. M. 1997, ApJ, 484, 628

Lovelace, R. V. E., & Romanova, M. M. 2003, ApJ, 596, L159

Lovelace, R. V. E., Romanova, M. M., & Newman, W. I. 1994, ApJ, 437, 136

Lovelace, R. V. E., Wang, J. C. L., & Sulkanen, M. E. 1987, ApJ, 315, 504

Lynden-Bell, D. 2003, MNRAS, 341, 1360

Romanova, M. M., & Lovelace R. V. E. 1997, ApJ, 475, 97

Romanova, M. M., Ustyugova, G. V., Koldoba, A. V., Chechetkin, V. M., & Lovelace, R. V. E. 1998, ApJ, 500, 703

Ustyugova, G. V., Lovelace, R. V. E., Romanova, M. M., Li, H., & Colgate, S. A. 2000, ApJ, 541, L21

Verboncoeur, J. P., Langdon, A. B., & Gladd, N. T. 1995, Comp. Phys. Comm., 87, 199

Zensus, J. A., Taylor, G. B., & Wrobel, J. M. 1998, in ASP Conf. Ser. 144, Radio Emission from Galactic and Extragalactic Compact Sources, ed. J. A. Zensus, G. B. Taylor, & J. M. Wrobel (San Francisco: ASP)

R. V. E. Lovelace and M. M. Romanova:Department of Astronomy, Space Science Building, Cornell University, Ithaca, New York 14853, USA (RVL1@cornell.edu).